CHAPTER 7
PHASED ARRAY RADAR ANTENNAS

Theodore C. Cheston
Naval Research Laboratory

Joe Frank
Technology Service Corporation

7.1 INTRODUCTION

Phased Array Radars

Multifunction Radar. Early radar systems used antenna arrays formed by the combination of individual radiators. Such antennas date back to the turn of the twentieth century.[1,2,3] Antenna characteristics are determined by the geometric position of the radiators and the amplitude and phase of their excitation. As radars progressed to shorter wavelengths, arrays were displaced by simpler antennas such as parabolic reflectors. For modern radar applications the advent of electronically controlled phase shifters and switches has once more directed attention to array antennas. The aperture excitation may now be modulated by controlling the phase of the individual elements to give beams that are scanned electronically. This chapter will be devoted to arrays of this type.

The capability of rapidly and accurately switching beams permits multiple radar functions to be performed, interlaced in time or even simultaneously. An electronically steered array radar may track a great multiplicity of targets, illuminate a number of targets with RF energy and guide missiles toward them, perform complete hemispherical search with automatic target selection, and hand over to tracking. It may even act as a communication system, directing high-gain beams toward distant receivers and transmitters. Complete flexibility is possible; search and track rates may be adjusted to best meet particular situations, all within the limitations set by the total use of time. The antenna beamwidth may be changed to search some areas more rapidly with less gain. Frequency agility is possible with the frequency of transmission changing at will from pulse to pulse or, with coding, within a pulse. Very high powers may be generated from a multiplicity of amplifiers distributed across the aperture. Electronically controlled array antennas can give radars the flexibility needed to perform all the various functions in a way best suited for the specific task at hand. The functions may be programmed adaptively to the limit of one's capability to exercise effective automatic management and control.

Phased array theory was studied intensively in the 1960s, bringing understanding. Technology advanced and led to a series of operational systems in the 1980s; many publications became available.[4–15] In terms of performance improvement, ultralow sidelobes (less than −40 dB) were demonstrated first in the 1970s by Westinghouse Electric Corporation's AWACS (Airborne Warning and Control System) and brought about tight tolerances in construction and phase settings. The advent of more and better computer modeling and sophisticated test equipment such as network analyzers has led to improved methods of designing well-matched apertures. Better components such as radiating elements, phase shifters, and power dividers are now available. More economical solid-state devices and memory chips have led to precision aperture phase control with corrections for frequency and temperature variations. Solid-state microwave devices hold great promise for future systems where a solid-state module is associated with each radiating element; improvements in terms of aperture control, reliability, and efficiency continue. Phased arrays can be controlled adaptively, particularly for sidelobe cancellation. This is an area where theory and understanding have advanced much. Also great progress has been made with indoor near-field antenna ranges,[16] where computer-controlled precision two-dimensional radiation patterns are derived at multiple frequencies, and with scanning.

Phased arrays are very expensive. As technology advances, costs are reduced, particularly in the areas of phase shifters and drivers. At the same time, the quest for better performance with lower sidelobes and wider bandwidth keeps the costs high. The greatest potential for cost reductions is believed to lie in the application of solid-state systems with a transmit/receive module at each element.

Phased Array Antennas. The phased array antenna has an aperture that is assembled from a great many similar radiating elements, such as slots or dipoles, each element being individually controlled in phase and amplitude. Accurately predictable radiation patterns and beam-pointing directions can be achieved.

The general planar array characteristics are readily obtained from a few simple equations, given here but discussed later in greater detail. With the elements spaced by $\lambda/2$ (λ = wavelength) to avoid the generation of multiple beams (grating lobes), the number of radiating elements N for a pencil beam is related to the beamwidth by

$$N \approx \frac{10{,}000}{(\theta_B)^2}$$

$$\theta_B \approx \frac{100}{\sqrt{N}}$$

where θ_B is the 3 dB beamwidth in degrees. The corresponding antenna gain, when the beam points broadside to the aperture, is

$$G_0 \approx \pi N \eta \approx \pi N \eta_L \eta_a$$

where η accounts for antenna losses (η_L) and reduction in gain due to unequal weighting of the elements with a nonuniform amplitude distribution (η_a). When scanning to an angle θ_0, the gain of a planar array is reduced to that of the projected aperture:

$$G(\theta_0) \approx \pi N \eta \cos \theta_0$$

Similarly, the scanned beamwidth is increased from the broadside beamwidth (except in the vicinity of endfire, $\theta_0 = 90°$):

$$\theta_B \text{ (scanned)} \approx \frac{\theta_B(\text{broadside})}{\cos \theta_0}$$

The total number of beams M (with broadside beamwidth and square stacking) that fit into a sphere is approximately equal to the gain and with $\eta \approx 1$ is thus simply related to N by

$$M \approx \pi N$$

In a planar array where the beamwidth changes with the scan angle, the number of beams that can actually be generated and fitted into a sphere is

$$M' \approx \frac{\pi}{2} N$$

An array where the elements are fed in parallel (Sec. 7.8) and which is scanned by phase shift, modulo 2π, has limited bandwidth since for wideband operation constant path lengths rather than constant phases are required. The limit is given by

$$\text{Bandwidth (\%)} \approx \text{beamwidth (deg)}$$

This is equivalent to limitations given by

$$\text{Pulse length} = 2 \times \text{aperture size}$$

With these criteria, the scanned radiation pattern at 60° is steered by ± one-fourth of the local scanned beamwidth as the frequency is changed over the band. If all the frequencies in the band are used with equal weighting, then twice the bandwidth (half the pulse length) becomes acceptable. At a scan angle θ_0 the beam steers with frequency through an angle $\Delta\theta$ so that

$$\delta\theta \approx \frac{\delta f}{f} \tan \theta_0 \qquad \text{rad}$$

For wider bandwidths, time-delay networks have to be introduced to supplement the phase shifters.

Conformal Arrays.[17,18] Phased arrays may conform to curved surfaces as required, for example, for flush-mounting on aircraft or missiles. If the surface has a large radius of curvature so that all the radiating elements point to substantially the same direction, then the characteristics are similar to those of a planar array even though the exact 3D position of the element has to be taken into account to calculate the required phase. A small radius of curvature is found with cylindrical (or spherical) arrays used for 360° coverage. Elements are switched to avoid sections of the antenna where they point away from the desired beam direction. Difficulties may be encountered in matching the radiating elements and in maintaining polarization purity. This geometry has not yet found use in radar systems.

The discussions in this chapter will concentrate on planar phased arrays.

3D Volumetric Search. 3D volumetric radar search is possible with electronic scanning in both azimuth and elevation; important regions (e.g., the horizon) may be emphasized at will and searched more frequently. The radar may operate with a higher than normal false-alarm rate since targets can easily be confirmed by repeated interrogation. Phase control allows beams to be widened, for example, to reduce search time for the more elevated regions, where reduced ranges need less antenna gain. A separate rotating surveillance radar system may be added for extra coverage (at a second frequency) and to allow more emphasis on tracking.

Monopulse Track. Phased array radars are well suited for monopulse tracking. The radiating elements of the array can be combined in three different ways to give the sum pattern and the azimuth and elevation difference patterns. Contradictory requirements in optimum amplitude distribution for sum and difference patterns exist,[19] but, as with other antenna systems, they may be independently satisfied. The sum and difference patterns are scanned simultaneously.

The difference-pattern null in a phased array system gives good beam-pointing accuracy. Absolute beam-pointing accuracies to within less than one-fiftieth of a (scanned) beamwidth have been measured with scans up to 60°.[20] The accuracy is limited by phase and amplitude errors. Since phase shift rather than time delay is used, as the frequency is changed, the direction of the null of the scanned beam is also changed, and the beam moves toward broadside with an increase in frequency. The amplitude at boresight of the difference-pattern output then increases linearly with a change in frequency. With a scan angle of 60° this change is from a null at the design frequency to a value of about −9 dB relative to the sum pattern, at the edge of the band, where the band is defined by bandwidth (percent) = beamwidth (deg). This is discussed more fully in Sec. 7.7.

Shaped Beams. The radiation pattern of an array may be shaped by modifying the aperture distribution. Good pattern approximations can be obtained by using phase only. In particular, the beam may be broadened by applying a spherical phase distribution to the aperture or by approximating it with a gable (triangular) phase distribution. Beams of this type are of particular interest since they are easily generated. They may be used for transmission in a system where the receiving antenna has a cluster of simultaneous beams, or, as previously discussed, they may be used in a search system to reduce the number of angular cells in regions of shorter range.

Monitoring. Electronically scanned arrays are composed of very many parts and include electronic circuitry to drive the phase shifters or switches that steer the beam. The overall reliability of such arrays can be great; graceful degradation has been claimed, since the failure of as much as 10 percent of the components leads to a loss in gain of only 1 dB. There is, however, a degradation of (low) sidelobes. Nevertheless, the functioning of the antenna is complex, and there is need for providing test or monitoring circuitry. The decision to point a beam in a certain direction is made somewhere in the radar control system and is normally defined by two direction cosines. A test or monitoring circuit should establish the correct functioning of all components, including all beam-pointing computations, electronic drivers and phase shifters or switches, and all their interconnections. Frequent indications that the antenna system is functioning or is capable of functioning should be available. In one possible method the phase shifters are programmed to focus on a nearby monitor probe and scan past it.[21] This will yield a close approximation of the complete radiation pattern, where gain and sidelobes can be measured and compared with previous results. The contribution of indi-

vidual elements and their phase shifters (and drivers) can also be checked with this configuration. The phase at each element is sequentially rotated at some low frequency; the amplitude and phase of this modulation as received by the probe relate directly to both the relative amplitude excitation of the element and its relative phase setting.[22] Other methods have been proposed[23] where measurements are compared with previously recorded ones.

Deployment of Apertures. With planar arrays, scanning is limited by the loss in gain and the increase in beamwidth corresponding to the reduction of the aperture to its projected area. Practical extreme values of scanning are therefore in the region of 60 to 70°. A minimum of three planar array apertures is then necessary for hemispherical coverage. For shipborne use, a minimum of four apertures appears desirable since, with pitch and roll, more than hemispherical coverage is necessary. The antennas may be positioned as shown in Fig. 7.1, permitting a view that is unimpeded by the central superstructure. The apertures would normally be tilted back from the vertical to balance the scan angles.

Radiating Elements. The most commonly used radiators for phased arrays are dipoles, slots, open-ended waveguides (or small horns), and printed-circuit "patches" (originally called *Collings radiator* after their inventor[24]). The element has to be small enough to fit in the array geometry, thereby limiting the element to an area of a little more than $\lambda^2/4$. In addition, many radiators are required, and the radiating element should be inexpensive and reliable and have identical characteristics from unit to unit.

Since the impedance and pattern of a radiator in an array are determined predominantly by the array geometry (Sec. 7.4), the radiating element may be chosen to suit the feed system and the physical requirements of the antenna. For example, if the radiator is fed from a stripline phase shifter, a stripline dipole

FIG. 7.1 Guided missile cruiser showing two out of four phased array antennas. (*Courtesy of Ingalls Shipbuilding Division of Litton.*)

would be a logical choice. If a waveguide phase shifter is used, an open-ended waveguide or a slot might be convenient. At the lower frequencies, where coaxial components are prevalent, dipoles have been favored. A ground plane is usually placed about $\lambda/4$ behind an array of parallel dipoles so that the antenna forms a beam in only one hemisphere. At the higher frequencies open-ended waveguides and slots are frequently used. Considerable bandwidth (perhaps 50 percent) can be obtained, even with patch radiators, provided they are fed similarly to a dipole.[25]

For limited scanning (say, less than 10°), it is possible to use directive radiators having dimensions of height and width of several wavelengths. With such separation, the mutual coupling effects can be small, and the pattern and impedance of an element in the array approach those of the isolated element.

The element must be chosen to give the desired polarization, usually vertical or horizontal. The special case of circular polarization is discussed below.

If polarization diversity is required or if an array is required to transmit one polarization and receive the orthogonal or both polarizations, either crossed dipoles or circular or square radiators seem suitable. With appropriate feed systems, both are capable of providing vertical and horizontal polarization independently and may be combined to provide any desired polarization, including circular. Such polarization diversity adds considerable complexity, requiring two feed systems or switches at the radiating element level.

Circular Polarization. From the point of view of the antenna designer, circular polarization is possible, though difficulties may be encountered in matching for large scan angles. On scanning, a component of the undesired orthogonal polarization will be generated,[26] and some provision should be made to absorb that energy.[27] With a conventional circularly polarized antenna, such as a parabolic dish with a circularly polarized feed, good circularity may be obtained over part of the main beam, with rapid deterioration over the rest of the pattern. With a planar array the relevant beamwidth is the beamwidth of the element in the array rather than the array beamwidth. The element beamwidth is broad, and good circularity may be expected over wide angles, including the main beam and sidelobes.

With circular polarization, the signal returned from a single-bounce target will require an antenna matched to the opposite sense of circular polarization from that transmitted. If the same antenna is used, then single-bounce targets are rejected. Such a system can therefore give a measure of suppression of rain echoes,[28] ideally amounting to

$$20 \log (e^2 + 1)/(e^2 - 1) \quad \text{dB}$$

where e is the voltage-ellipticity ratio. An early model of a Raytheon reflectarray gave an ellipticity ratio of less than 1.5 dB with scans up to 30°, corresponding to a theoretical rain rejection of at least 15 dB. At the same time, an aircraft target would typically lose approximately 3 dB, leaving a relative net improvement of 12 dB of rain rejection.

Phased Arrays with Very Wide Bandwidth. A radar system that has the capability of changing frequency over a very wide band can, with advantage, adapt its transmission to take into account frequency-dependent multipath characteristics, target response, environmental conditions, interference, and jamming. Further, wideband processing can give fine range resolution.

Phased arrays have the potential of operating over very wide bandwidths. Some ferrite phase shifters operate over two octaves,[29] and digital diode phase shifters that switch line lengths may function over even wider bands. The high

end of the frequency band is limited by the physical size of the elements, which must be spaced close enough in the array to avoid the generation of grating lobes. For wide instantaneous bandwidth (rather than tunable bandwidth), time delays have to be added to prevent the beam from being scanned as the frequency is changed.

The impedance of the radiating element at the aperture (with closely spaced elements) is approximately independent of frequency, but the element must be matched over the wide band. This is difficult to achieve without exciting harmful surface waves when scanning. Nevertheless, matching with octave bandwidth for scanning to $\pm 60°$ appears possible.

Limited Scanning.[30] If scanning is limited to a small angular volume, considerable simplifications become possible. The total number of active phase-shifter controls can be reduced to about equal the total number of beams. Subarrays may be formed, each with only one phase control and of a size such that its beamwidth includes all the scan angles. Alternatively, a small phased array could be placed in the focal region of a large reflector to scan the narrow beamwidth of the reflector over a limited scan angle.

Scanning of Arrays

Phase Scanning. The beam of an antenna points in a direction that is normal to the phase front. In phased arrays, this phase front is adjusted to steer the beam by individual control of the phase of excitation of each radiating element. This is indicated in Fig. 7.2*a*. The phase shifters are electronically actuated to permit rapid scanning and are adjusted in phase to a value between 0 and 2π rad. With an interelement spacing s, the incremental phase shift ψ between adjacent elements for a scan angle θ_0 is $\psi = (2\pi/\lambda)s \sin \theta_0$. If the phase ψ is constant with frequency, the scan angle θ_0 is frequency-dependent.

Time-Delay Scanning. Phase scanning was seen to be frequency-sensitive. Time-delay scanning is independent of frequency. Delay lines are used instead of

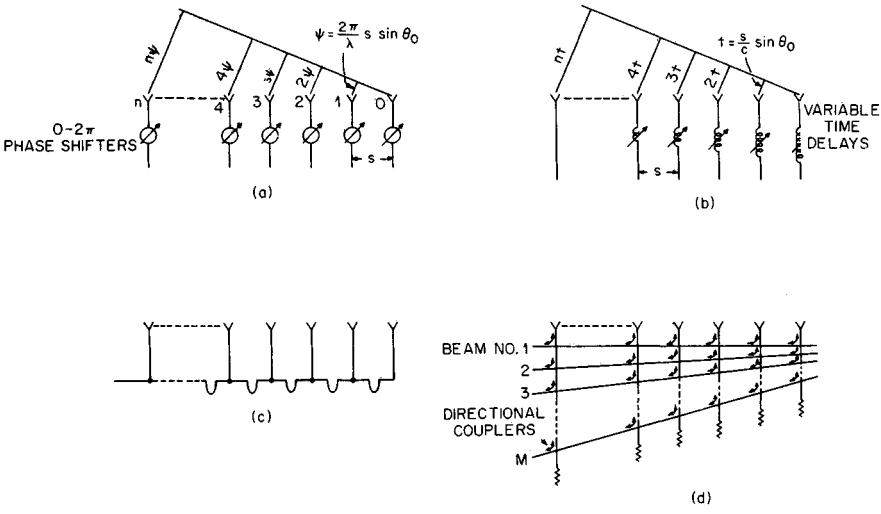

FIG. 7.2 Generation of scanned beams. (*a*) Phased array. (*b*) Time-delay array. (*c*) Frequency-scanned array. (*d*) Blass-type array.

phase shifters, as shown in Fig. 7.2*b*, providing an incremental delay from element to element of $t = (s/c) \sin \theta_0$, where c = velocity of propagation. Individual time-delay circuits (Sec. 7.7) are normally too cumbersome to be added to each radiating element. A reasonable compromise may be reached by adding one time-delay network to a group of elements (subarray) where each element has its own phase shifter.

Frequency Scanning.[31] Frequency rather than phase may be used as the active parameter to exploit the frequency-sensitive characteristics of phase scanning. Figure 7.2*c* shows the arrangement. At one particular frequency all radiators are in phase. As the frequency is changed, the phase across the aperture tilts linearly, and the beam is scanned. Frequency-scanning systems are relatively simple and inexpensive to implement. They have been developed and deployed in the past to provide elevation-angle scanning in combination with mechanical horizontal rotation for 3D radars. A chapter in the first edition of this handbook was devoted to this approach, which since then has received much less attention; frequency is usually considered too important a parameter to give up for scanning.

IF Scanning. For receiving, the output from each radiating element may be heterodyned (mixed) to an intermediate frequency (IF). All the various methods of scanning are then possible, including the beam-switching system described below, and can be carried out at IF, where amplification is readily available and lumped constant circuits may be used.

Digital Beamforming.[32–34] For receiving, the output from each radiating element may be amplified and digitized. The signal is then transferred to a computer for processing, which can include the formation of multiple simultaneous beams (formed with appropriate aperture illumination weighting) and adaptively derived nulls in the beam patterns to avoid spatial interference or jamming. Limitations are due to the availability and cost of analog-to-digital (A/D) converters and to their frequency and dynamic-range characteristics. Partial implementation is possible by digitizing at subarray levels only.

Beam Switching. With properly designed lenses or reflectors, a number of independent beams may be formed by feeds at the focal surface. Each beam has substantially the gain and beamwidth of the whole antenna. Allen[35] has shown that there are efficient equivalent transmission networks that use directional couplers and have the same collimating property. A typical form, after Blass,[36] is shown in Fig. 7.2*d*. The geometry can be adjusted to provide equal path lengths, thus providing frequency-independent time-delay scanning. Another possible configuration providing multiple broadband beams uses parallel plates containing a wide-angle microwave lens[37,38] (Gent, Rotman). Each port corresponds to a separate beam. The lens provides appropriate time delays to the aperture, giving frequency-invariant scanning. The beams may be selected through a switching matrix requiring $M-1$ single-pole–double-throw (SPDT) switches to select one out of M beams. The beams are stationary in space and overlap at about the 4 dB points. This is in contrast to the previously discussed methods of scanning, where the beam can be steered accurately to any position. The beams all lie in one plane. The system may be combined with mechanical rotation of the antenna, giving vertical switched scanning for 3D coverage. Much greater complexity is required for a system switching beams in both planes.

Multiple Simultaneous Beams. Instead of switching the beams, as described in the preceding paragraph, all the beams may be connected to separate receivers, giving multiple simultaneous receive beams. The transmitter radiation pattern would need to be wide to cover all the receive beams. Such multibeam sys-

tems have found application in combination with mechanical rotation for 3D coverage.

Multiple Independently Steered Beams. Independent multiple beams may be generated with a single beamformer by modifying both amplitude and phase at the aperture. This can be seen from Fig. 7.3, where, for example, two independent beams are generated. Both beams have the same amplitude (voltage) distribution $F(x)$ but differently inclined linear phased fronts. The total aperture excitation with both beams is

$$F(x,\psi) = F(x)e^{j2\psi_1(x/a)} + F(x)e^{j2\psi_2(x/a)} = 2F(x)\left[\cos(\psi_1 - \psi_2)\frac{x}{a}\right]e^{j(\psi_1+\psi_2)(x/a)}$$

That is, the aperture amplitude distribution required for two separate beams varies cosinusoidally, and the phase distribution is linear and has the average inclination.

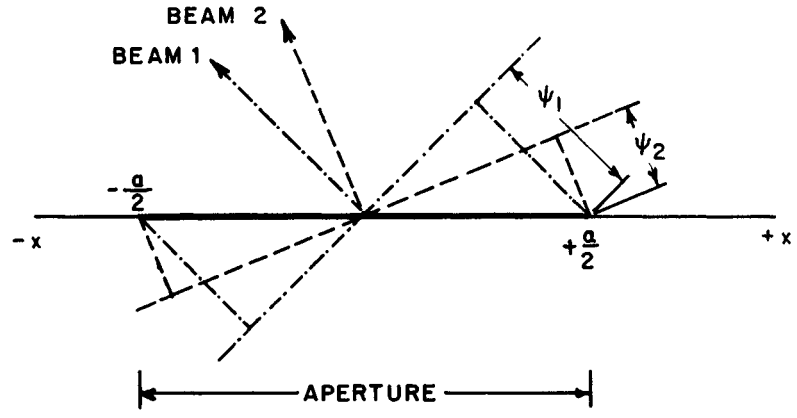

FIG. 7.3 Aperture distribution giving two beams.

In most phased array systems only the phase can be controlled. Ignoring the required amplitude variations still leads to good approximations for forming multiple beams, by superimposing the various required phase-shifter settings (modulo 2π). In the case of two beams, the aperture phase slope has the average inclination and varies periodically from 0 to π.

It should be noted that when a multilobed radiation pattern is received or transmitted in one channel, the gain is shared between the lobes. When the beams are contained in separate (beamforming) channels, however, each channel has the full gain of the aperture.

Vertical Scan Only. A greatly simplified phased array system becomes possible if there is no need for multifunction capabilities, including fire control, where a beam may have to be pointed in any given direction at any time. The array is scanned in the vertical plane only and mechanically rotated to give azimuth coverage. The number of phase control points is then reduced to the number of horizontal rows. In the case of a ship's surveillance radar, the antenna should be positioned as high as possible to avoid shadowing by the superstruc-

ture, but the pedestal need not be stabilized since stabilization can be achieved by electronic beam steering. Scanning can be in the form of phase scanning or beam switching, or multiple simultaneous beams may be used on receive with a wide antenna pattern on transmit. Many systems of this type have been developed for both naval and land-based use (Sec. 7.11).

7.2 ARRAY THEORY

Array with Two Elements. Figure 7.4 shows two isotropic radiators which are spaced by a distance s and excited with equal amplitude and phase. With unity input power, the vector sum of their contributions, added at a great distance as a function of θ, is the radiation pattern

$$E_a(\theta) = \frac{1}{\sqrt{2}}\left[e^{j(2\pi/\lambda)(s/2)\sin\theta} + e^{-j(2\pi/\lambda)(s/2)\sin\theta}\right]$$

where θ is measured from the broadside direction. Normalizing, to give unity amplitude when $\theta = 0$, and simplifying give

$$E_a(\theta) = \cos\left[\pi \frac{s}{\lambda}\sin\theta\right] \tag{7.1}$$

The absolute value of $E_a(\theta)$ is plotted in Fig. 7.4 as a function of $\pi(s/\lambda)\sin\theta$. If the plot had been in terms of the angle θ, the lobes would have been found to increase in width as $|\theta|$ increased. The main lobe occurs when $\sin\theta = 0$. The other lobes have the same amplitude as the main lobe and are referred to as *grating lobes*. They occur at angles given by $\sin\theta = \pm [m/(s/\lambda)]$, where m is an integer. For the half space given by $-90° < \theta < +90°$, there are $2m'$ grating lobes, where m' is the largest integer smaller than s/λ. If $s < l$, grating-lobe maxima do not occur, and the value at $\pm 90°$ is $\cos(\pi s/\lambda)$. This value is for isotropic radiators and is reduced if the radiators have directivity.

Linear Array.[39] With a linear array of N isotropic radiators, excited with equal amplitudes and phase and separated by distances s, as shown in Fig. 7.5, the condition for the occurrence of grating lobes is unchanged from the simpler case just considered. They occur for the same values of $\pi(s/\lambda)\sin\theta$, but the width of the lobes is reduced, and they are separated by minor lobes. Summing the vector contributions from all elements, with element 0 as phase reference, gives

$$E_a(\theta) = \frac{1}{\sqrt{N}} \sum_{n=0}^{n=N-1} e^{j(2\pi/\lambda)\, ns\sin\theta}$$

The factor $1/\sqrt{N}$ shows that each element is energized with $1/N$ of the (unity) input power. Normalizing the gain to unity at broadside, $\theta = 0$, gives the pattern

$$E_a(\theta) = \frac{\sin[N\pi(s/\lambda)\sin\theta]}{N\sin[\pi(s/\lambda)\sin\theta]} \tag{7.2}$$

$E_a(\theta)$ gives the radiation pattern for isotropic radiators and is known as the *array factor*. It is shown in Fig. 7.6 for $N = 10$. The pattern is repetitive, and the lo-

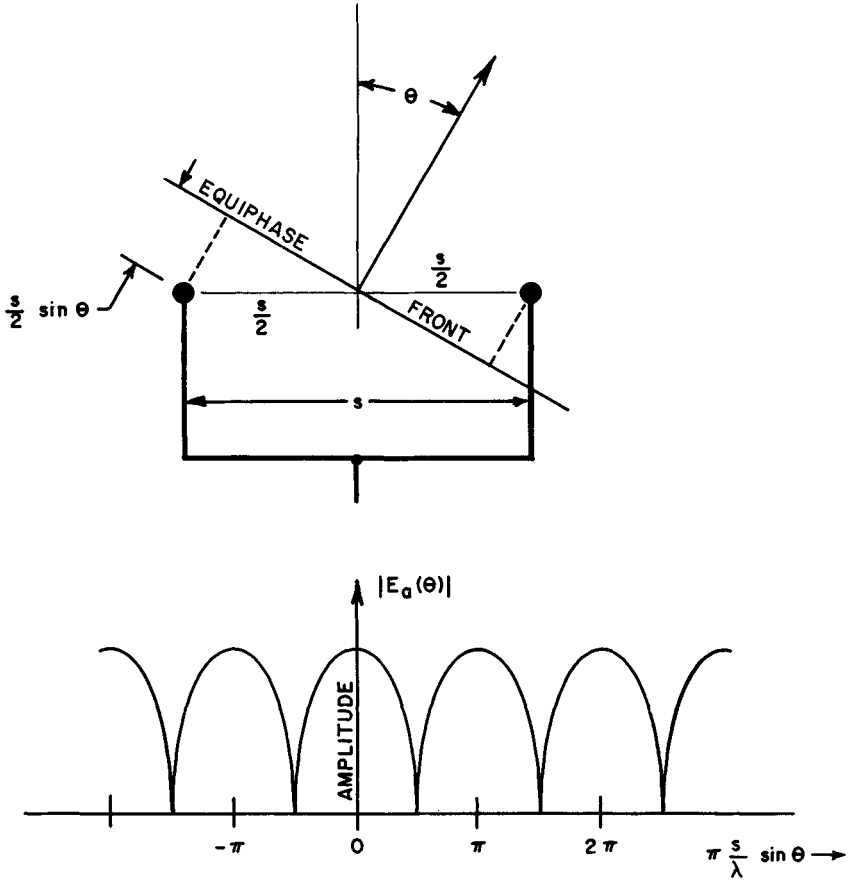

FIG. 7.4 Radiation pattern of two isotropic radiators.

cations of the adjacent grating lobes at angles θ_1 and θ_2 are separated by $\pi(s/\lambda)$ $(\sin\theta_1 - \sin\theta_2) = \pi$.

The radiating elements are not isotropic but have a radiation pattern $E_e(\theta)$, known as the *element factor* or *element pattern*; then the complete radiation pattern $E(\theta)$ is the product of the array factor and the element pattern:

$$E(\theta) = E_e(\theta)E_a(\theta) = E_e(\theta)\frac{\sin\left[N\pi(s/\lambda)\sin\theta\right]}{N\sin\left[\pi(s/\lambda)\sin\theta\right]} \tag{7.3}$$

An approximation to the pattern of Eq. (7.2) is in the form

$$E(\theta) = \frac{\sin\left[\pi(a/\lambda)\sin\theta\right]}{\pi(a/\lambda)\sin\theta} \tag{7.4}$$

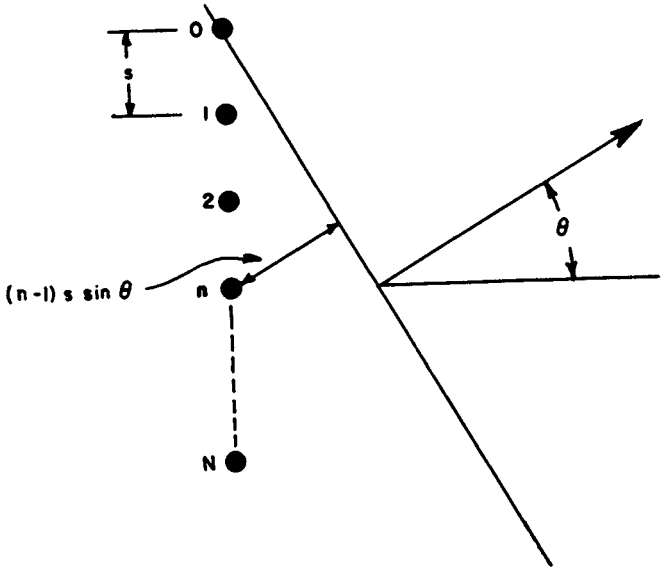

FIG. 7.5 Linear array with N radiators uniformly spaced by a distance s.

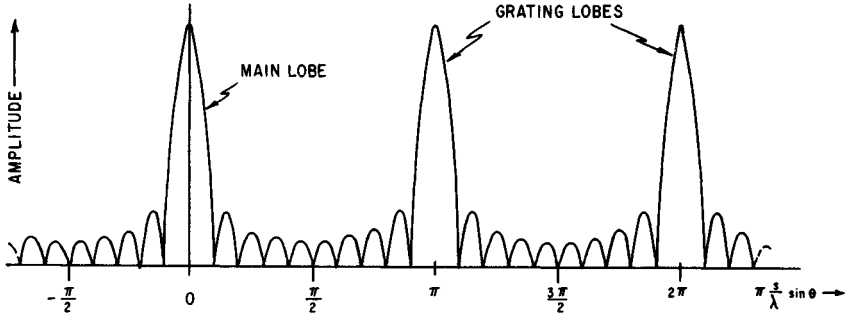

FIG. 7.6 Array factor with $N = 10$ elements.

where the effective aperture is $a = Ns$, which extends by $s/2$ beyond the centers of the end elements. In contrast to the array factor, this pattern has only one maximum and is nonrepetitive. It is the well-known Fourier transform of a continuous constant-amplitude distribution and is a reasonable approximation for small values of θ when the aperture is greater than several wavelengths. The *half-power beamwidth* is obtained from Eq. (7.4):

$$\theta_B = \frac{0.886}{a/\lambda} \text{ (rad)} = \frac{50.8}{a/\lambda} \text{ (deg)} \tag{7.5}$$

The first sidelobe is 13.3 dB down from the peak of the main beam.

For larger values of θ the pattern of a continuous aperture is modified from Eq. (7.4) by the obliquity factor[40,41] $\frac{1}{2}(1 + \cos\theta)$, which arises from the definition of a Huygens source. This gives

$$E(\theta) = \tfrac{1}{2}(1 + \cos\theta)\frac{\sin[\pi(a/\lambda)\sin\theta]}{\pi(a/\lambda)\sin\theta} \tag{7.6}$$

For closely spaced elements the obliquity factor is very similar to the amplitude pattern of a well-designed (matched) radiating element, $\sqrt{\cos\theta}$ for values up to some 60 or 70°. At greater angles the element pattern has values that are greater than those given by $\sqrt{\cos\theta}$ and that are a function of the total number of elements.[42]

Scanned Linear Arrays. The pattern of the array may be steered to an angle θ_0 by applying linearly progressive phase increments from element to element so that the phase between adjacent elements differs by $2\pi(s/\lambda)\sin\theta_0$. Equation (7.2) is then modified, giving the normalized array factor of a uniformly illuminated array as

$$E_a(\theta) = \frac{\sin N\pi(s/\lambda)(\sin\theta - \sin\theta_0)}{N\sin\pi(s/\lambda)(\sin\theta - \sin\theta_0)} \tag{7.7}$$

and the pattern is

$$E(\theta) = E_e(\theta)\frac{\sin N\pi(s/\lambda)(\sin\theta - \sin\theta_0)}{N\sin[\pi(s/\lambda\sin\theta]} \tag{7.8}$$

Equation (7.8) describes the fundamental response of a scanned array system. The array factor will have only one single major lobe, and grating-lobe maxima will not occur for $-90° < \theta < +90°$ as long as

$$\pi\frac{s}{\lambda}|\sin\theta - \sin\theta_0| < \pi$$

or

$$\frac{s}{\lambda} < \frac{1}{1 + |\sin\theta_0|} \tag{7.9}$$

which is always true if $s/\lambda < \frac{1}{2}$. When scanning is limited, the value of s/λ may be increased, for example, to $s/\lambda < 0.53$ for scanning to a maximum of 60° or to $s/\lambda < 0.59$ for scanning to a maximum of ±45°.

For larger values of s/λ, grating lobes occur at angles θ_1, given by

$$\sin\theta_1 = \sin\theta_0 \pm \frac{n}{s/\lambda} \tag{7.10}$$

where n is an integer.

In the limit, the inequality (7.9) does allow a grating-lobe peak to occur at 90° when scanning to θ_0. Even though the grating lobe is reduced when multiplied by

the element pattern, it may be prudent to space the elements such that the first null of the grating lobe, rather than the peak, occurs at 90°. With N elements this more restrictive condition is given by

$$\frac{s}{\lambda}\frac{N-1}{N} \times \frac{1}{1+|\sin\theta_0|} \tag{7.11}$$

Equation (7.8) may again be approximated by the Fourier transform of the illumination across the continuous aperture:

$$E(\theta) = \tfrac{1}{2}(1+\cos\theta)\frac{\sin \pi(a/\lambda)(\sin\theta - \sin\theta_0)}{\pi(a/\lambda)(\sin\theta - \sin\theta_0)} \tag{7.12}$$

The Fourier-transform solutions for continuous apertures[19,43] may be used to approximate patterns for practical amplitude and phase distributions as long as the element-to-element spacing is small enough to suppress grating lobes.[44] *Monopulse difference patterns* may be approximated in the same way from the Fourier transforms of the corresponding continuous odd aperture distributions. For example, with a constant amplitude distribution, the difference-pattern array factor calculated by the exact vector addition of all radiating elements is

$$E_a(\theta) = \frac{1 - \cos N\pi(s/\lambda)(\sin\theta - \sin\theta_0)}{N \sin \pi(s/\lambda)(\sin\theta - \sin\theta_0)}$$

The Fourier transform gives the same expression with the *sine* in the denominator replaced by its argument, giving (in the denominator) $\pi(a/\lambda)(\sin\theta - \sin\theta_0)$, where $a = Ns$.

For small scan angles θ_0 and small values of θ the expression $\sin\theta - \sin\theta_0$ may be approximated by $\theta - \theta_0$. For larger values of θ_0, the expression $\sin\theta - \sin\theta_0$ may be expanded to give the response in the general direction of the (narrow) scanned beam in terms of the *small angle* $(\theta - \theta_0)$:

$$\sin\theta - \sin\theta_0 \approx a\theta - \theta_0)\cos\theta_0 \tag{7.13}$$

This gives, with Eq. (7.12),

$$E(\theta) \not\approx \tfrac{1}{2}(1+\cos\theta)\frac{\sin[(\pi a\cos\theta_0)/\lambda](\theta - \theta_0)}{[(\pi a\cos\theta_0)/\lambda](\theta - \theta_0)} \tag{7.14}$$

Equation (7.14) measures the angle $\theta - \theta_0$ from the scanned direction. It shows that the effect of scanning is to reduce the aperture to the size of its projected area in the direction of scan. Correspondingly, the beamwidth is increased to

$$\theta_B \text{ (scanned)} \not\approx \frac{\theta_B \text{ (broadside)}}{\cos\theta_0} = \frac{0.886}{(a/\lambda)\cos\theta_0} \text{ (rad)} = \frac{50.8}{(a/\lambda)\cos\theta_0} \text{ (deg)} \tag{7.15}$$

When the beam is scanned from broadside by an angle $\theta_0 < 60°$ and the aperture

$a/\lambda \geq 5$, Eq. (7.15) gives a beamwidth that is too narrow, the error being less than 7 percent.

When the beam is scanned to very large scan angles, toward endfire, more exact calculations become necessary.[42,45] Equation (7.8) still applies and gives, for endfire with isotropic radiators,

$$\theta_B \text{ (endfire)} = 2\sqrt{\frac{0.886}{a/\lambda}} \text{ rad} \tag{7.16}$$

Element Factor and Gain of Planar Arrays. The gain of a uniformly illuminated and lossless aperture of area A, with a broadside beam, is $G_{(o)} = 4\pi A/\lambda^2$. With a nonuniform aperture distribution and with losses present, the gain is reduced by the efficiency term η to

$$G_{(0)} = 4\pi \frac{A}{\lambda^2} \eta \tag{7.17}$$

If the aperture is considered as a matched receiver, then the amount of energy arriving from a direction θ_0 is proportional to its projected area. The gain with scanning therefore is

$$G(\theta_0) = 4\pi \frac{A \cos \theta_0}{\lambda^2} \eta \tag{7.18}$$

The variation of gain with the cosine of the scan angle agrees with the equivalent variation in beamwidth given by Eq. (7.15). The gain may be expressed in terms of the actual beamwidth, giving, from Eqs. (7.15) and (7.18),

$$G(\theta_0) \not\approx \frac{32{,}000}{\theta_B \phi_B} \eta \tag{7.19}$$

where θ_B and ϕ_B are the beamwidths in degrees in the two principal planes with the beam scanned to θ_0.

If the aperture is made up of N equal radiating elements and is matched to accept the incident power, then the contribution to the overall gain is the same from all elements, whence

$$G(\theta) = NG_e(\theta)\eta \tag{7.20}$$

where G_e is the gain per element. It follows from Eq. (7.18) that the matched-element power pattern is

$$G_e(\theta) = 4\pi \frac{A}{N\lambda^2} \cos \theta \tag{7.21}$$

and the normalized radiation amplitude pattern of the (matched) element or (matched) *element pattern* is

$$E_e(\theta) = \sqrt{\cos \theta} \tag{7.22}$$

It has already been noted that the matched-element pattern is very similar to the obliquity factor ½(1 + cos θ) and differs markedly only near endfire, where the number of elements begins to matter.[42]

For a given element spacing s the total number of radiators N in the area A is $N = A/s^2$, and Eq. (7.21) gives

$$G_e(\theta) = 4\pi \left[\frac{s}{\lambda}\right]^2 \cos \theta$$

When the element spacing is $s = \lambda/2$, then the power pattern of an element that is perfectly matched at all scan angles is

$$G_e(\theta) = \pi \cos \theta \tag{7.23}$$

and the peak antenna gain in the direction of scan, θ_0, is

$$G(\theta_0) = \pi N \eta \cos \theta_0 \tag{7.24}$$

where the efficiency term η accounts for losses and for a nonuniform aperture distribution. For a broadside beam $\theta_0 = 0$ and

$$G_0 = \pi N \eta \tag{7.25}$$

and the element gain is $G_e = \pi$.

The effects of the element pattern are most marked with wide beams. Figure 7.7 shows the array and element factors and the resulting pattern for a 10-element array, with element spacing $s = \lambda/2$, scanned to 60°. The pattern maximum is noted to occur at less than 60° because the gain of the element pattern increases toward broadside. The pattern value at 60° is cos 60° = 0.5 in power or 0.707 in amplitude, relative to the maximum at broadside, as expected. The sidelobes in the general region of broadside are not reduced since in that region the element

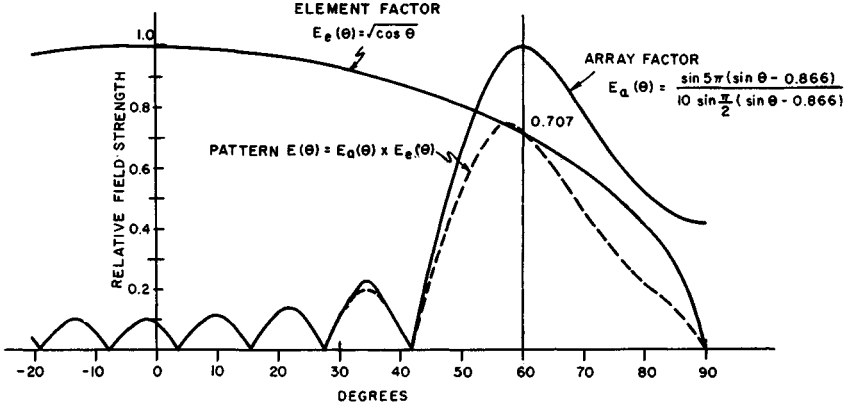

FIG. 7.7 Ten-element linear array scanned to 60°. Element spacing $s = \lambda/2$.

pattern is approximately unity. Relative to the beam maximum, therefore, the sidelobes near broadside are increased by approximately 3 dB.

7.3 PLANAR ARRAYS AND BEAM STEERING

Planar Arrays. A planar array is capable of steering the beam in two dimensions. In a spherical-coordinate system the two coordinates θ and ϕ define points on the surface of a unit hemisphere. As shown in Fig. 7.8, θ is the angle of scan measured from broadside and ϕ is the plane of scan measured from the x axis. Von Aulock[46] has presented a simplified method for visualizing the patterns and the effect of scanning. He considers the projection of the points on a hemisphere onto a plane (Fig. 7.9); the axes of the plane are the direction cosines $\cos \alpha_x$, $\cos \alpha_y$. For any direction on the hemisphere the direction cosines are

$$\cos \alpha_x = \sin \theta \cos \phi$$
$$\cos \alpha_y = \sin \theta \sin \phi$$

The direction of scan is indicated by the direction cosines $\cos \alpha_{xs}$, $\cos \alpha_{ys}$. Here the plane of scan is defined by the angle ϕ measured counterclockwise from the $\cos \alpha_x$ axis and is given by

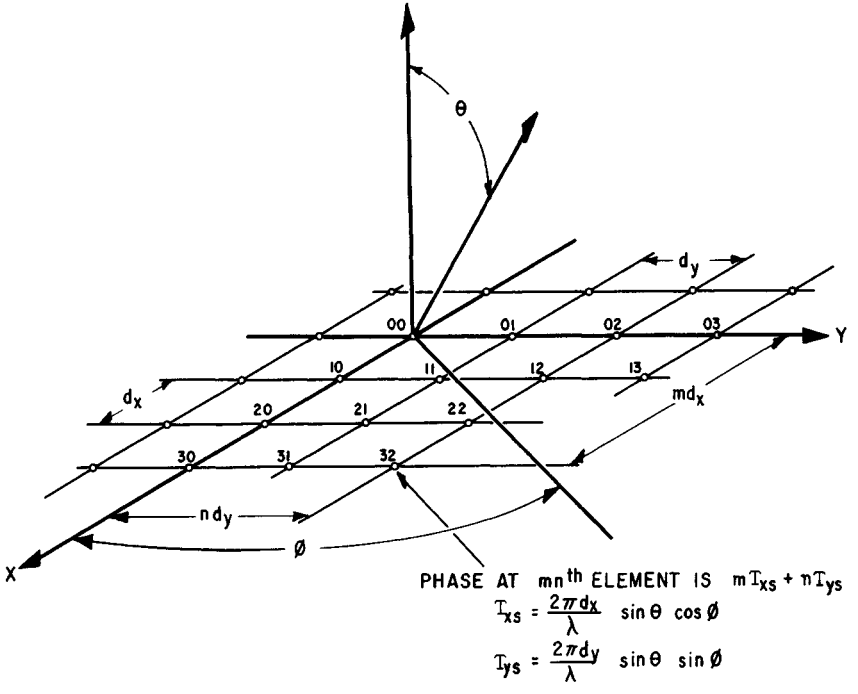

FIG. 7.8 Planar-array-element geometry and phasing.

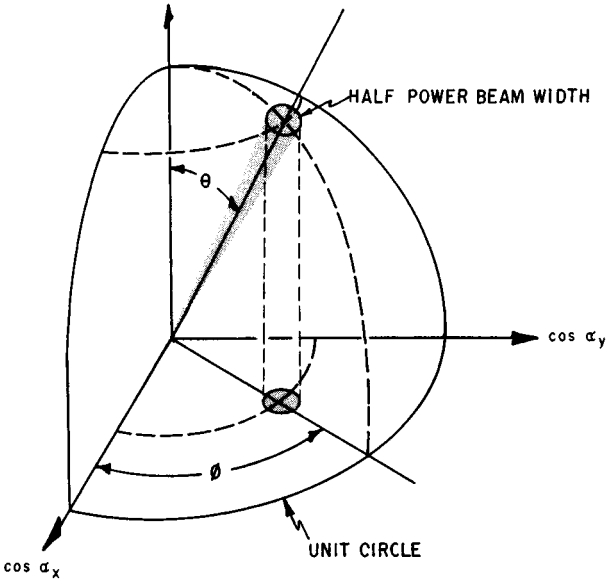

FIG. 7.9 Projection of points on a hemisphere onto the plane of the array.

$$\phi = \tan^{-1}\frac{\cos \alpha_{ys}}{\cos \alpha_{xs}}$$

The angle of scan θ is determined by the distance of the point (cos α_{xs}, cos α_{ys}) from the origin. This distance is equal to sin θ. For this reason a representation of this sort is called sin θ space. A feature of sin θ space is that the antenna pattern shape is invariant to the direction of scan. As the beam is scanned, every point on the plot is translated in the same direction and by the same distance as is the beam maximum.

The region inside the unit circle where

$$\cos^2 \alpha_x + \cos^2 \alpha_y \leq 1$$

is defined as *real space*, the hemisphere into which energy is radiated. The infinite region outside the unit circle is referred to as *imaginary space*. Although no power is radiated into imaginary space, the concept is useful for observing the motion of grating lobes as the array is scanned. In addition, the pattern in imaginary space represents stored energy and contributes to the element impedance in the array.

The most common element lattices have either a rectangular or a triangular grid. As shown in Fig. 7.8, the *mn*th element is located at (md_x, nd_y). The triangular grid may be thought of as a rectangular grid where every other element has been omitted. The element locations can be defined by requiring that $m + n$ be even.

Calculations for the element-steering phases are greatly simplified by the

adoption of the direction cosine coordinate system. In this system the linear-phase tapers defined by the beam-steering direction ($\cos \alpha_{xs}$, $\cos \alpha_{ys}$) may be summed at each element so that the phasing at the mnth element is given by

$$\psi_{mn} = mT_{xs} + nT_{ys}$$

where $T_{xs} = (2\pi/\lambda)d_x \cos \alpha_{xs}$ = element-to-element phase shift in the x direction
$T_{ys} = (2\pi/\lambda)d_y \cos \alpha_{ys}$ = element-to-element phase shift in the y direction

The array factor of a two-dimensional array may be calculated by summing the vector contribution of each element in the array at each point in space. For an array scanned to a direction given by the direction cosines $\cos \alpha_{xs}$ and $\cos \alpha_{ys}$, the array factor of an $M \times N$ rectangular array of radiators may be written

$$E_a(\cos \alpha_{xs}, \cos \alpha_{ys}) = \sum_{m=0}^{M-1} \sum_{n=0}^{N-1} |A_{mn}| e^{j[m(T_x - T_{xs}) + n(T_y - T_{ys})]}$$

where $T_x = (2\pi/\lambda)\, d_x \cos \alpha_x$
$T_y = (2\pi/\lambda)\, d_y \cos \alpha_y$
A_{mn} = amplitude of mnth element

An array may be visualized as having an infinite number of grating lobes only one of which (namely, the main beam) is desired in real space. It is convenient to plot the position of the grating lobes when the beam is phased for broadside and observe the motion of these lobes as the beam is scanned. Figure 7.10 shows the grating-lobe locations for both rectangular and triangular spacings. For a rectangular array the grating lobes are located at

$$\cos \alpha_{xs} - \cos \alpha_x = \pm \frac{\lambda}{d_x} p$$
$$\cos \alpha_{ys} - \cos \alpha_y = \pm \frac{\lambda}{d_y} q$$
$$p, q = 0, 1, 2, \ldots$$

The lobe at $p = q = 0$ is the main beam. A triangular grid is more efficient for suppressing grating lobes than a rectangular grid,[47] so that for a given aperture size fewer elements are required. If the triangular lattice contains elements at (md_x, nd_y), where $m + n$ is even, the grating lobes are located at

$$\cos \alpha_{xs} - \cos \alpha_x = \pm \frac{\lambda}{2d_x} p$$
$$\cos \alpha_{ys} - \cos \alpha_y = \pm \frac{\lambda}{2d_y} q$$

where $p + q$ is even.

Since only one main lobe is normally desired in real space, an appropriate design will place all but one maximum in imaginary space for all angles of scan. With scanning, lobes that were originally in imaginary space may move into real space if the element spacing is greater than $\lambda/2$. As the array is scanned away from broadside, each grating lobe (in $\sin \theta$ space) will move a distance equal to the sine of the angle of scan and in a direction determined by the plane of scan. To ensure that no grating lobes enter real space, the element spacing must be

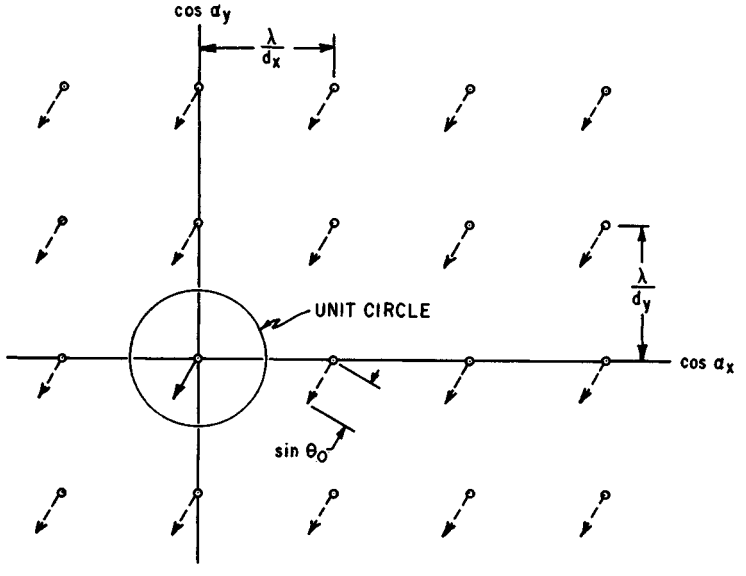

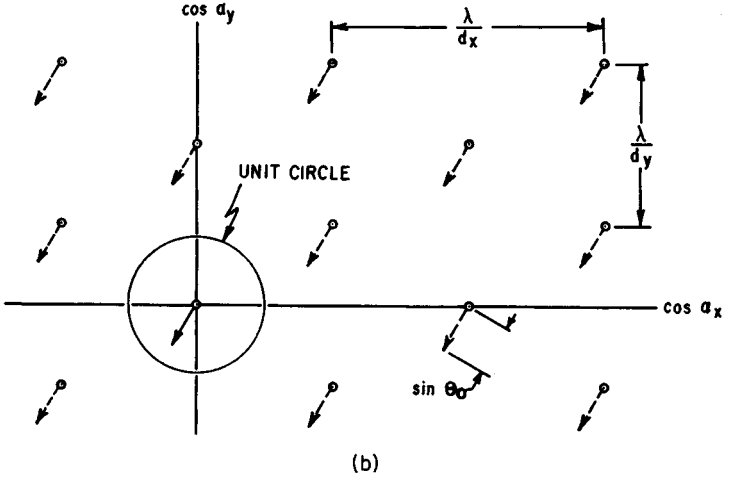

FIG. 7.10 Grating-lobe positions for (*a*) rectangular and (*b*) triangular grids, showing the motion of the lobes as the beam is scanned an angle θ_o.

chosen so that for the maximum scan angle θ_m the movement of a grating lobe by $\sin \theta_m$ does not bring the grating lobe into real space. If a scan angle of 60° from broadside is required for every plane of scan, no grating lobes may exist within a circle of radius $1 + \sin \theta_m = 1.866$. The square grid that meets this requirement has

$$\frac{\lambda}{d_x} = \frac{\lambda}{d_y} = 1.866 \quad \text{or} \quad d_x = d_y = 0.536\lambda$$

Here, the area per element is

$$d_x d_y = (0.536\lambda)^2 = 0.287\lambda^2$$

For an equilateral-triangular array, the requirement is satisfied by

$$\frac{\lambda}{d_y} = \frac{\lambda}{\sqrt{3}\, d_x} = 1.866 \quad \text{or} \quad d_y = 0.536\lambda \quad d_x = 0.309\lambda$$

Since elements are located only at every other value of mn, the area per element is

$$2d_x d_y = 2(0.536\lambda)(0.309\lambda) = 0.332\lambda^2$$

For the same amount of grating-lobe suppression, the square geometry requires approximately 16 percent more elements.

Element-Phasing Calculations. A computer is usually required to perform the steering computations for a phased array antenna. It can compensate for many of the known phase errors caused by the microwave components, the operating environment, and the physical placement of the elements. For example, if the insertion and differential phase variations (which may occur from phase shifter to phase shifter) are known, they may be taken into account in the computations. Known temperature variations across the array that would induce phase errors may be compensated for. Finally, many feeds (e.g., optical and series feeds) do not provide equal phase excitation at the input to each phase shifter. The relative phase excitation caused by these feeds is a known function of frequency. In these cases, the computer must provide a correction based on the location of the element in the array and on the frequency of operation.

For a large array with thousands of elements, many calculations are required to determine the phasing of the elements. These calculations must be performed in a short period of time. The use of the orthogonal phase commands mT_{xs}, nT_{ys} helps to minimize these calculations. Once the element-to-element phase increments T_{xs}, T_{ys} have been computed for a given beam-pointing direction, the integral multiples of T_{ys} may be used to steer the columns (Fig. 7.8). If an adder is located at each element, the row-and-column values mT_{xs} and nT_{ys} may be summed at the element. It is also possible to put two phase shifters in series so that the summation can be done at microwave frequencies. This may be implemented with the use of a series feed, as shown in Fig. 7.11. Here the row steering commands apply equally to all rows. An amplifier between a row phase shifter and a series feed is desirable so that the generated power does not have to take the loss of two phase shifters in series. In addition, the row phase shifters must be capable of accurate phasing. Since relatively few row phase shifters are required, it is reasonable to make them considerably more accurate than the phase shifters in the array. Any corrections for a phase taper

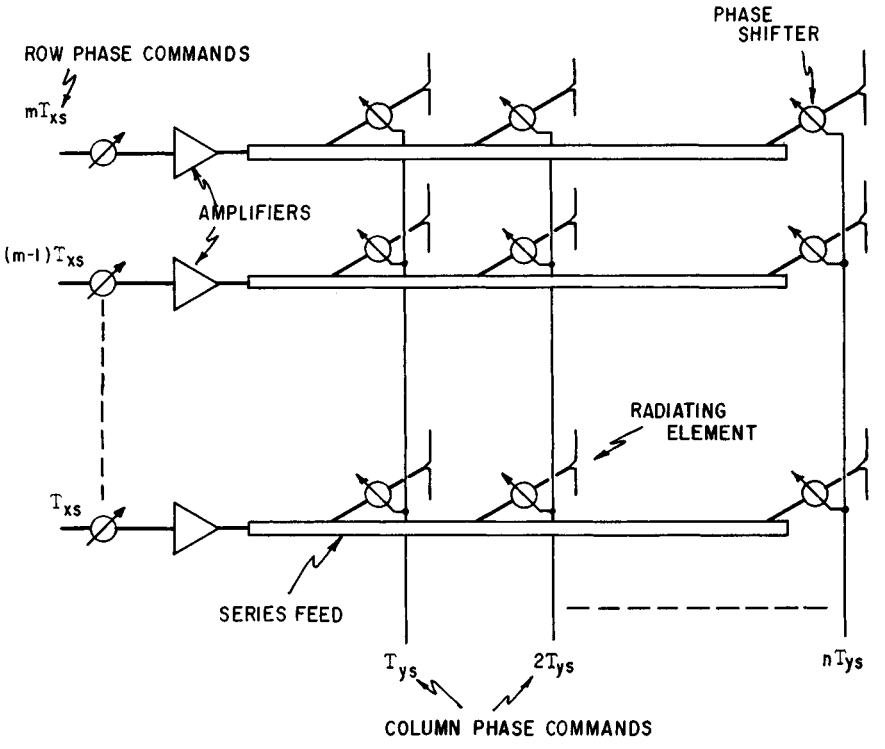

FIG. 7.11 Microwave addition of orthogonal phasing commands by means of a series feed.

across the series feed may be applied for an entire column if all the feeds have the same phase characteristics.

A large array requires many electronic phase-shifter drivers and very complex wiring to provide control signals and energy. The problem is complicated by the relatively close spacing of elements in the array. Further, many phase shifters are of the digital type and require a driver and control signal for each bit. The problems are eased somewhat in the system described above with two RF phase shifters in series, since many elements may use the same steering commands and the same drivers. In other systems it may be necessary to provide each element in the array with an independent phase command. The command may include a phase correction for the correction of errors due to component tolerances. An adder at each element provides rapid steering through the use of row-and-column steering commands. If high-speed phase shifting is not required, the computer may compute sequentially and store the phases for each of the elements. All the phase commands can then be delivered simultaneously.

7.4 APERTURE MATCHING AND MUTUAL COUPLING[48]

Significance of Aperture Matching. An antenna is a device that acts as a transformer to provide a good match between a source of power and free

space. If the antenna is not matched to free space, power will be reflected back toward the generator, resulting in a loss in radiated power. In addition, a mismatch produces standing waves on the feed line to the antenna. The voltage at the peaks of these standing waves is $(1 + |\Gamma|)$ times greater than the voltage of a matched line, where Γ is the voltage reflection coefficient. This corresponds to an increased power level that is $(1 + |\Gamma|)^2$ times as great as the actual incident power. Therefore, while the antenna is radiating less power, individual components must be designed to handle more peak power. With antennas that do not scan, the mismatch may often be tuned out by conventional techniques, preferably at a point as close to the source of the mismatch as possible.

In a scanning array the impedance of a radiating element varies as the array is scanned, and the matching problem is considerably more complicated. Unlike a conventional antenna, where mismatch affects only the level of the power radiated and not the shape of the pattern, spurious lobes in the scanning array may appear as a consequence of the mismatch. Further, there are conditions where an antenna that is well matched at broadside may have some angle of scan at which most of the power is reflected.

The variation in element impedance and element pattern is a manifestation of the mutual coupling between radiating elements that are in close proximity to one another. For a practical design, two empirical techniques are of great value:

1. Waveguide simulators provide a means for determining the element impedance in an infinite array with the use of only a few elements. The effectiveness of a matching structure based on these measurements may also be determined in the simulator.

2. A small array is the best technique for determining the active element pattern. The active element pattern, obtained by exciting one element and terminating its neighbors, is the best overall measure of array performance other than the full array itself. If a large reflection occurs at some angle of scan, it can be recognized by a null in the element pattern. The small array can also provide data on the coupling between elements. This data can be used to calculate the variation in impedance as the array is scanned.

Both these techniques will be discussed later in this section.

Effects of Mutual Coupling. When two antennas (or elements) are widely separated, the energy coupled between them is small and the influence of one antenna on the current excitation and pattern of the other antenna is negligible. As the antennas are brought closer together, the coupling between them increases. In general, the magnitude of the coupling is influenced by the distance between the elements, the pattern of the elements, and the structure in the vicinity of the elements. For example, the radiation pattern of a dipole has a null in the $\theta = \pm 90°$ direction and is omnidirectional in the $\theta = 0°$ plane. Therefore it can be expected that dipoles in line will be loosely coupled and parallel dipoles will be tightly coupled. When an element is placed in an array of many elements, the effects of coupling are sufficiently strong that the pattern and impedance of the element in the array are drastically altered.

The terms *active element pattern* and *element impedance* refer to an element in its operating environment (i.e., in an array with its neighboring elements excited). In the array, each excited element couples to every other element. The coupling from several elements to a typical central element, element 00, is shown in Fig. 7.12. The $C_{mn,pq}$ are mutual-coupling coefficients relating the voltage (amplitude and phase) induced in the *mn*th element to the voltage excitation at the

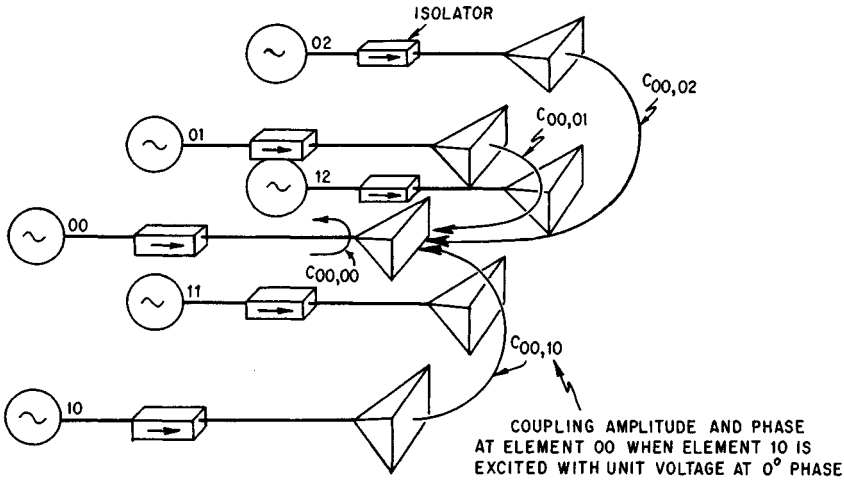

FIG. 7.12 Coupled signals to a central element from neighboring elements.

*pq*th element. The coupled signals add vectorially to produce a wave traveling toward the generator of element 00 that appears to be a reflection from the radiator of element 00. As the phases of the neighboring elements are varied to scan the beam, the vector sum of the coupled signals changes and causes an apparent change in the impedance of element 00. For some scan angles the coupled voltages tend to add in phase, causing a large reflection and possibly the loss of the main beam. Large reflections often occur at scan angles just prior to the emergence of a grating lobe into real space, but in some instances such reflections may occur at smaller scan angles.

The description of the impedance variation given above made no reference to the feed network or the phase shifters and assumed that the only coupling between elements is via the radiating aperture. The coupling coefficients would be measured, and by superposition the phased-voltage contributions from every element in the array (or at least those in the immediate vicinity) would be added vectorially to produce the voltage reflected back toward the generator. In a practical array the impedance variation depends upon the feed system and the phase shifter. If these are taken into account, the impedance variation may be different from what the above model might predict. In most analyses only the coupling at the aperture is considered. This description provides insight into the intrinsic impedance variation of the aperture when it is isolated from other effects, as in the case where each element has an independent feed (e.g., its own generator and isolator). In this case it is a simple matter to measure the voltage–standing-wave ratio (VSWR) in any line and determine exactly the extent of the impedance and mismatch variation. For many feed systems this is not possible, and a measurement of the reflected energy will provide erroneous information and a false sense of security. Unless all the reflections are collimated back at some central point (or independent feeds are used), some of the reflected energy will generally be re-reflected and contribute to large undesirable sidelobes.

For large arrays the impedance of an element located near the center of the array is often taken as typical of the impedance of every element in the array. As might be expected, this element is most strongly influenced by elements in its immediate vicinity. When the array is scanned, the influence of elements several

wavelengths distant is also significant. For dipoles above a ground plane the magnitude of the coupling between elements decays rapidly with distance. For a reasonable indication of array performance, an element in the center of a 5 by 5 array may be taken as typical of an element in a large array. For dipoles with no ground plane (or the dual, slots in a ground plane) the coupling between elements does not decay so rapidly, and a 9 by 9 array appears reasonable. For an array of open-ended waveguides, a 7 by 7 array should suffice (see Fig. 7.22, below). If accurate prediction of the array performance is required, many more elements are needed than are indicated above.[49,50]

It is often convenient to assume that the array is infinite in extent and has a uniform amplitude distribution and a linear-phase taper from element to element. In this manner every element in the array sees exactly the same environment, and the calculations for any element apply equally to all. These assumptions provide a significant simplification in the calculation of the element impedance variations. In addition, impedance measurements made in simulators correspond to the element impedance in an infinite array. In spite of the assumptions, the infinite-array model has predicted with good accuracy the array impedance and the impedance variations. Even arrays of modest proportions (less than 100 elements) have been in reasonable agreement with the results predicted for an infinite array.[51]

Element Pattern. From energy considerations the directional gain of a perfectly matched array with constant amplitude distribution ($\eta = 1$) will vary as the projected aperture area, from Eq. (7.18)

$$G(\theta_0) = \frac{4\pi A}{\lambda^2} \cos \theta_0$$

If it is assumed that each of the N elements in the array shares the gain equally, the gain of a single element is [Eq. (7.21)]

$$G_e(\theta) = \frac{4\pi A}{N\lambda^2} \cos \theta_0$$

If the element is mismatched, having a reflection coefficient $\Gamma(\theta, \phi)$ that varies as a function of scan angle, the element gain pattern is reduced to

$$G_e(\theta) = \frac{4\pi A}{N\lambda^2} (\cos \theta)[1 - |\Gamma(\theta, \phi)|^2]$$

The element pattern is seen to contain information pertaining to the element impedance.[52–55] The difference between the total power radiated in the element pattern and the power delivered to the antenna terminals must equal the reflected power. In terms of the radiation patterns of the scanning array, this means that since the scanned antenna patterns trace out the element pattern, it follows that the average power lost from the scanned patterns is equal to the power lost from the element pattern because of reflections. It is not enough to match one element in the presence of all its terminated neighbors. The element will deliver power to its neighbors, and this loss in power corresponds to the average power lost when scanning. An ideal although not necessarily realizable element pattern would place all the radiated power into the scan region, giving a pattern like a cosine on a pedestal and thereby providing maximum antenna gain for the number of elements used.

Thinned Arrays. The number of radiating elements in an array may be reduced to a fraction of those needed completely to fill the aperture without suffering serious degradation in the shape of the main beam. However, average sidelobes are degraded in proportion to the number of elements removed. The element density may be thinned so as to effectively taper the amplitude distribution, and the spacing is such that no coherent addition can occur to form grating lobes. A thinned aperture, where elements have been removed randomly from a regular grid,[56] is shown in Fig. 7.13. The gain is that due to the actual number of elements $NG_e(\theta)$, but the beamwidth is that of the full aperture. For example, if the array has been thinned so that only 10 percent of

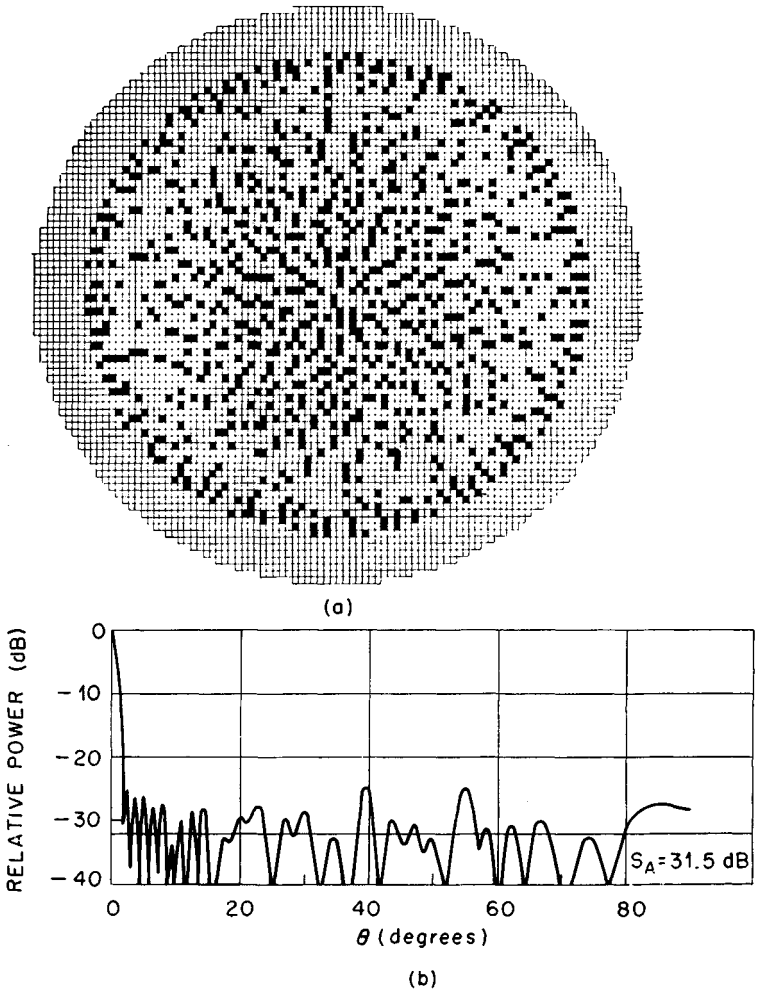

FIG. 7.13 (*a*) Thinned array with a 4000-element grid containing 900 elements. (*b*) Typical pattern for a thinned array. S_A is the average sidelobe level. (*From Willey,*[56] *courtesy of Bendix Radio.*)

the elements are used, the gain of the array will drop by 10 dB. However, since the main beam is virtually unchanged, about 90 percent of the power is delivered to the sidelobe region.

If the removed elements (in a regular thinned array) are replaced with elements with matched loads, the element pattern is identical to that of one in the regular array with all elements excited. The element pattern is independent of the array excitation, and the same fractional amount of power will be lost (because of mismatch) whether the array is thinned, tapered, or uniformly illuminated. It should be noted that the concept of an element pattern that applies equally to every element is valid only when isolating feeds are used and edge effects are ignored.

A thinned array may also be implemented with an irregular element spacing, although this is not common. In this case the element gain (and impedance) will vary from element to element, depending upon the environment of a given element. To obtain the gain of the array, it is necessary to sum all the different element gains $G_{en}(\theta)$. Thus

$$G(\theta) = \sum_n G_{en}(\theta)$$

Impedance Variation of Free Space. It is of interest to examine the case of a large continuous aperture which may be considered to be the limiting case of an array of many very small elements.[57] The free-space impedance E/H varies as cos θ for scanning in the E plane and as sec θ for scanning in the H plane. The impedance of a medium is thus dependent upon the direction of propagation, and the impedance variation of a scanning aperture is a natural consequence of this dependence. The continuous aperture appears to represent a lower limit to the impedance variation with scanning. This is indicated by Allen's results,[58] where the impedance variation with scanning was calculated for dipoles above a ground plane. In spite of increased mutual coupling, or perhaps because of it, the more closely the dipoles were spaced, the smaller the impedance variation with scanning (Fig. 7.14). Although the impedance variation decreased, the absolute impedance of the dipoles also decreased, making them more difficult to match at broadside. It is expected that to obtain an impedance variation smaller than that of free space some impedance compensation must be employed.

Element Impedance. The simplest and most straightforward method for computing the variation in reflection coefficient (and impedance) is by means of the scattering matrix of mutual-coupling coefficients. The mutual-coupling coefficients may be easily measured for elements of all types by exciting one element and terminating each of the other elements in a matched load. The ratio of the induced voltage at element mn to the excitation voltage at element pq gives the amplitude and phase of the coupling coefficient $C_{mn,pq}$. Once these coefficients are determined, it is a simple matter to compute the mismatch for any set of phasing conditions.

Consider the two-element array shown in Fig. 7.15 where each element is provided with an isolating feed. The incident wave in each element is represented by V_1, V_2, and the total reflected wave in each element is represented by V_1', V_2'. It should be apparent that the total reflected wave in any element

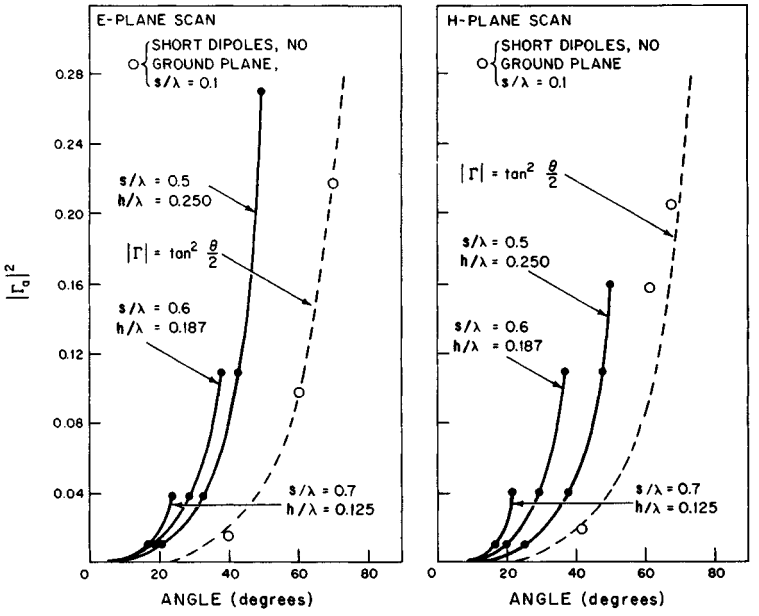

FIG. 7.14 Scanned mismatch variation for different element spacings (h/λ is the dipole spacing above a ground plane). (*After Allen.*[58])

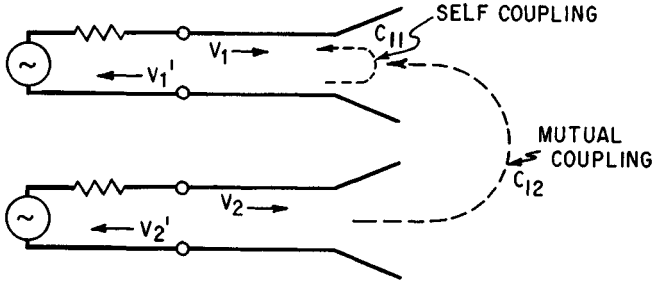

FIG. 7.15 Scattering-matrix model for a two-element array.

is the vector sum of the couplings from all elements, including its own reflection as a self-coupling:

$$V_1' = C_{11} V_1 + C_{12} V_2$$

$$V_2' = C_{21} V_1 + C_{22} V_2$$

The reflection coefficient in each element is obtained by dividing the reflected voltage by the incident voltage in the channel:

$$\Gamma_1 = \frac{V_1'}{V_1} = C_{11} \frac{V_1}{V_1} + C_{12} \frac{V_2}{V_1}$$

$$\Gamma_2 = \frac{V_2'}{V_2} = C_{21}\frac{V_1}{V_2} + C_{22}\frac{V_2}{V_2}$$

Note that all the quantities must contain both phase and amplitude and that as the phases of V_1, V_2 are varied to scan the beam, the reflection coefficients (Γ_1, Γ_2) will vary. Although only two elements have been used in this example, the technique is completely general. For a large array the reflection coefficient of the *mn*th element is given by

$$\Gamma_{mn} = \sum_{\text{all } pq} C_{mn,pq}\frac{V_{pq}}{V_{mn}}$$

The general case is treated in more detail by Oliner and Malech.[59] No restrictions need be placed on either the amplitude or the phase of the excitation at each element. There are also no restrictions on the spacing between the elements as long as the coupling coefficients are measured for the spacing and environment to be used. A considerable simplification is obtained by assuming that each of the elements sees the same environment and has the same voltage excitation. Then $|V_{pq}|/|V_{mn}|$ will always be unity, and the reflection coefficient at element *mn* is merely the sum of the mutual-coupling coefficients with the excitation phase at each element taken into account:

$$\Gamma_{mn} = \sum_{\text{all } pq} C_{mn,pq}e^{j(m-p)T_{xs}}e^{j(n-q)T_{ys}}$$

where $e^{j(m-p)T_{xs}}$ and $e^{j(n-q)T_{ys}}$ give the relative phase excitations in the x and y directions of the *pq*th element with respect to the *mn*th element. The impedance variation relative to a matched impedance at broadside may be obtained immediately from

$$\frac{Z_{mn}(\theta,\phi)}{Z_{mn}(0,0)} = \frac{1 + \Gamma_{mn}(\theta,\phi)}{1 - \Gamma_{mn}(\theta,\phi)}$$

Analytical Techniques. Stark[60] presents a thorough description of analytical techniques and insight to the problem of mutual coupling. He derives necessary and sufficient conditions for array blindness (i.e., nulls in the active element pattern). Evidence is provided to demonstrate that more closely spaced elements reduce the variation of impedance due to scanning in spite of the increase in mutual coupling.

Elliott and coworkers[61,62] have developed design procedures for slot arrays which are fed by either air-filled or dielectric-filled waveguide. These procedures take into account the differences in mutual coupling for central elements in an array as well as for the edge elements. This is particularly of interest when designing a small array.

Munk and colleagues[63,64] have developed a procedure for reducing the variations in impedance with scanning by matching elements with dielectric slabs. Their analytical results show a VSWR of less than 1.5 for scan angles of ±80° in

each of the principal planes. The penalty they incur for placing a thick (0.4λ) and potentially heavy dielectric slab in front of the aperture is mitigated by the low dielectric constant of the slab ($\epsilon_r = 1.3$). This suggests that a lightweight loaded foam material could be used. Dielectric slabs on the surface of an array can often create surface waves and array blindness. In this case, however, the dielectric constant is quite low. The surface wave can be avoided by spacing the elements more closely. Here, as in some other cases, it is seen that closely spaced elements are beneficial for improving impedance matching for scanning arrays. Obviously, reducing the element spacing increases the number of elements and hence the cost without any increase in gain or reduction in beamwidth.

Another very useful tool for the computation of the impedance variation with scanning is the grating-lobe series,[65,66] which describes the impedance variation of an infinite array of regularly spaced elements.

Nonisolating Feeds. When nonisolating feeds are used, the mutual-coupling effects become dependent on whether the phase-shifting element is reciprocal or nonreciprocal. Figure 7.16 shows a space-fed array where it is assumed that the initial excitations at the input aperture are of equal amplitude and phase. If the phase shifters are nonreciprocal, the round-trip phase of a signal reflected from the radiating aperture is independent of phase-shifter setting. Therefore, when reflections occur at the radiating aperture, the reflected signal is phased so that the input aperture appears as a mirror as seen from the feed side, with the magnitude of the reflection being determined by the radiating aperture. Since the reflected beam does not scan, it should be possible to provide a good match at the input aperture. Matching the input aperture, in this case, is equivalent to providing the radiating aperture with independent feeds. Any secondary reflection from the input aperture will radiate in the original direction of scan.

If reciprocal phase shifters are used, the energy reflected from the radiating aperture will pick up equal additional phase shift on reflection from the radiating aperture, resulting in a beam at the input aperture that is phased to scan to twice the original scan angle (in sin θ space). Some energy will undergo secondary re-

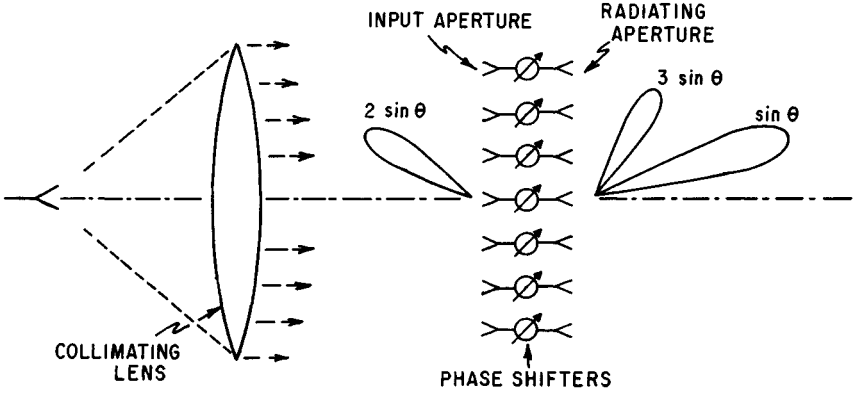

FIG. 7.16 Nonisolating feed showing spurious lobes when reciprocal phase shifters are used.

flection from the input aperture (which now has a mismatch corresponding to a scan of 2 sin θ) and will be phase-shifted once again to produce a beam at the radiating aperture in the direction 3 sin θ. Additional reflections acquire twice the original phase shift for each round trip, resulting in radiated beams at positions of 5 sin θ, 7 sin θ, etc. The magnitude of these beams is approximately equal to the product of the voltage reflection coefficients if the number of bounces is taken into account. For example, let $\Gamma_r(\sin\theta)$, $\Gamma_f(2\sin\theta)$ denote the reflection coefficients corresponding to scan angles of sin θ at the radiating aperture and 2 sin θ at the input aperture. If $\Gamma_r(\sin\theta) = 0.2$ and $\Gamma_f(2\sin\theta) = 0.5$, the magnitude of the radiated lobe directed at 3 sin θ would be $\Gamma_r(\sin\theta)\,\Gamma_f(2\sin\theta) = 0.1$, or 20 dB down from the main lobe. Similar results can be expected from series feeds[67] and from reactive parallel feeds.[48]

Mutual Coupling and Surface Waves. The mutual coupling between two small isolated dipoles[68] should decrease as $1/r$ in the H plane and $1/r^2$ in the E plane (E and H planes are interchanged for slots). Coupling measurements[69] have shown that in the array environment the rate of decay is slightly greater than predicted above, indicating that some of the energy is delivered to other elements in the array and may be dissipated and reradiated from these elements. The same measurements have shown that the phase difference of the energy coupled to elements is directly proportional to their distance from the excited elements, indicative of a surface wave traveling along the array, leaking energy to each of the elements. For best performance the velocity of the surface wave should be very close to that of free space. If the array contains waveguides or horns loaded with dielectric, the velocity will decrease slightly. Further, if the dielectric protrudes from the radiators or if a dielectric sheet is used in front of the array, the velocity of the surface wave may decrease dramatically. This surface wave is important since it can cause a large reflection (and an accompanying loss of the beam) for some angles of scan. This can best be seen by examining the condition of phasing for which the couplings from many elements will add in phase to cause a large reflection in a typical element.

Consider an array in which the velocity of the surface wave is that of free space. The difference in the phase of the voltages coupled from an adjacent pair of elements to element 00 (Fig. 7.17) is related to the scan angle by

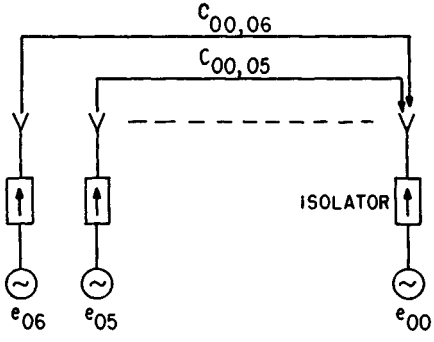

FIG. 7.17 Two adjacent elements coupling to another element in the same row.

$$\Delta\chi = \frac{2\pi s}{\lambda} + \frac{2\pi s}{\lambda}\sin\theta_0 = \frac{2\pi s}{\lambda}(1 + \sin\theta_0)$$

The couplings will be in phase when $\Delta\psi = 2\pi$ or when

$$\frac{s}{\lambda} = \frac{1}{1 + \sin\theta_0}$$

This is seen to be exactly the same condition as previously determined for the emergence of a grating lobe into real space. Therefore, it may be expected that when a grating lobe is about to emerge into real space, the coupled voltages tend to add in phase and cause a large mismatch. If the dielectric protrudes from the aperture or if a dielectric sheet covers the aperture (this is one technique for scan compensation discussed below), a large reflection may occur well before the grating lobe reaches real space.[70] If a surface-wave velocity of v_s is assumed, the couplings will add in phase when

$$\frac{s}{\lambda} = \frac{1}{c/v_s + \sin\theta_0}$$

For the purposes of mutual coupling, a slow wave across the aperture may be envisioned as being equivalent to spacing the elements farther apart in free space.

A phenomenon that produces similar effects can come about without dielectric in front of the aperture, e.g., by using a periodic structure of baffles. Under certain conditions an array of open-ended waveguides will perform as though a slow wave were propagating across the aperture. This effect has been analyzed and studied experimentally,[71,72] and it has been shown that as the array is scanned, higher-order modes are excited in the waveguides. Even though these modes are cut off, they contribute to the active impedance. At certain angles, almost all the energy is reflected, causing a null in the element pattern. To guard against these reflections it is best to design the radiators so that higher-order modes are well into the cutoff region. Figure 7.18 shows the results obtained by Diamond,[72] using a waveguide array. When only the dominant TE_{10} mode was taken into account, the null could not be explained. When the TE_{20} mode (which was only slightly cut off) was taken into account, the null showed up clearly. Since a null in the element pattern indicates in-phase addition of the mutually coupled signals, it appears that the array of open-ended waveguides causes the couplings between elements to have a phase variation corresponding to a velocity slower than that of free space.

Regardless of the cause of the null, it will show up in the element pattern. If only a few elements surround the central element, the null will normally be shallow and broad. If many elements are used, the null will be deep and sharp. The null will also show up if the mutual-coupling coefficients are measured and used to calculate the reflection coefficient.

Array Simulators. A good deal of effort has gone into matching a radiator in the presence of an array of radiators. The use of waveguide simulators as developed by Wheeler Laboratories has made it possible to determine the matching structure experimentally without the need of building an array. A waveguide, operating in a TE_{10} mode, may be considered to contain two inclined-plane waves propagating down the guide. The angle that each of the plane waves makes with the longitudinal direction (Fig. 7.19) is determined by

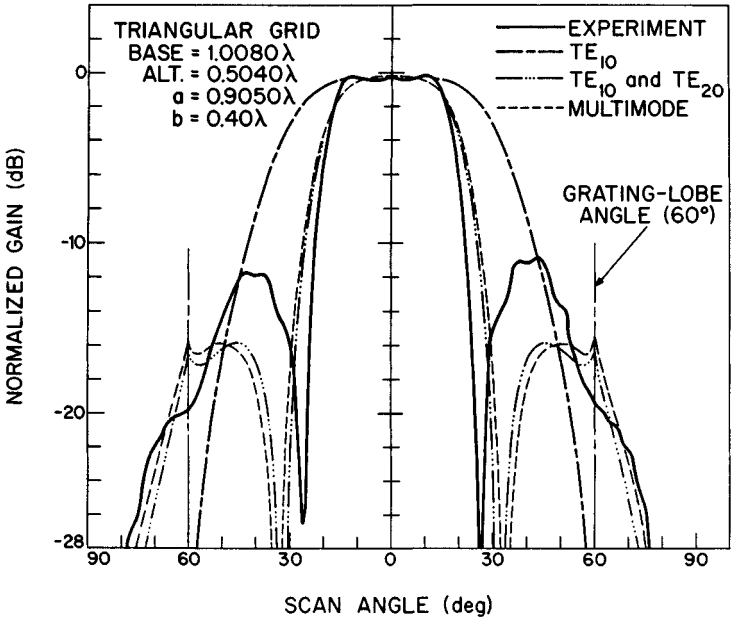

FIG. 7.18 Comparison of the theoretical and an experimental *H*-plane element pattern: triangular array of waveguides with a 2:1 ratio of width to height. (*From Diamond.*[72])

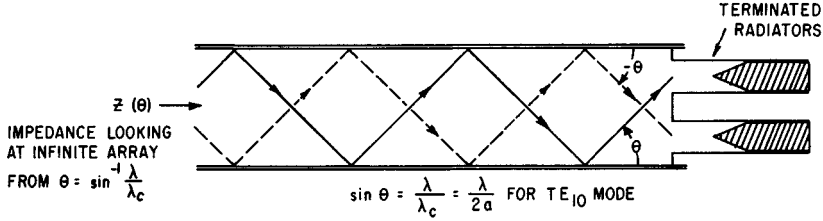

FIG. 7.19 Array simulator terminated with two dummy elements.

the *H* dimension of the waveguide and simulates the angle of scan of an infinite array:

$$\sin \theta = \frac{\lambda}{\lambda_c} \tag{7.26}$$

where θ = scan angle
λ = free-space wavelength
λ_c = cutoff wavelength of guide

Additional scan angles may be simulated by exciting other modes. The waveguide dimensions are chosen so that a radiating element or elements placed

in the waveguide sees mirror images in the walls of the waveguide that appear to be at the same spacing as the array to be simulated. Both rectangular and triangular arrays may be simulated, as shown in Fig. 7.20. The impedance measurements are made by looking into a waveguide simulator that is terminated with dummy elements. This is equivalent to looking at an infinite array from free space at a scan angle given by Eq. (7.26). A matching structure, designed from the simulator impedance data, may be placed into the simulator to measure its effectiveness. Several simulator designs, results, and a complete discussion of the topic have been presented by Hannan and Balfour.[73] The technique is limited in that only discrete scan angles can be simulated. Several scan angles in both planes of scan give a general idea of the array impedance but may miss a large reflection of the type described in this section under "Mutual Coupling and Surface Waves." Nevertheless, the array simulator is the best method available for empirically determining the array impedance without building an array.

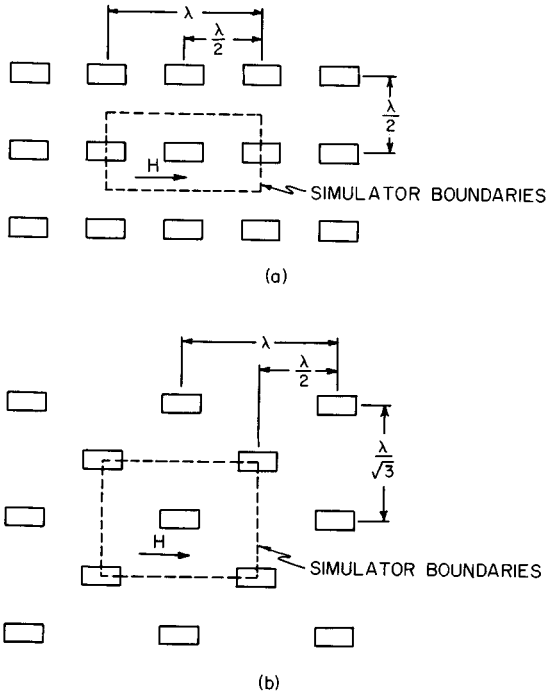

FIG. 7.20 Rectangular- and triangular-array geometries with simulator boundaries superimposed. (*a*) Square array with simulator superimposed. (*b*) Triangular array with simulator superimposed.

Under certain conditions, the matched element impedance may be determined analytically by envisioning a simulator.[74] For example, if the waveguide simulator is terminated by a single dummy element, the matched impedance of the element is exactly the impedance of the waveguide. Since waveguide impedances are well known, the matched impedance at the simulator scan angle is also known.

Compensation for Scanned Impedance Variation. The impedance of an element in an array has been discussed and has been shown to vary as the array is scanned. An array that is matched at broadside can be expected to have at least a 2:1 VSWR at a 60° angle of scan. To compensate for the impedance variation, it is necessary to have a compensation network that is also dependent on scanning.

One method uses a thin sheet of high-dielectric-constant material (e.g., alumina) spaced a fraction of a wavelength from the array, as shown in Fig. 7.21.This is in contrast to the method used by Munk[63,64] and described under "Analytical Techniques." The properties of a thin dielectric sheet (less than a quarter wave in the medium) are such that to an incident plane wave it appears as a susceptance that varies with both the plane of scan and the angle of scan. Magill and Wheeler[75] describe the technique in greater detail and present the results of a particular design using simulators. An alumina matching sheet is attractive because it simultaneously provides a natural radome. It should be cautioned that a dielectric sheet in front of the aperture may produce a slow surface wave and a possible null in the element pattern. However, a thin dielectric matching sheet has been used for a 400-element array,[51] and some compensation has been achieved without any noticeable slow-wave phenomenon.

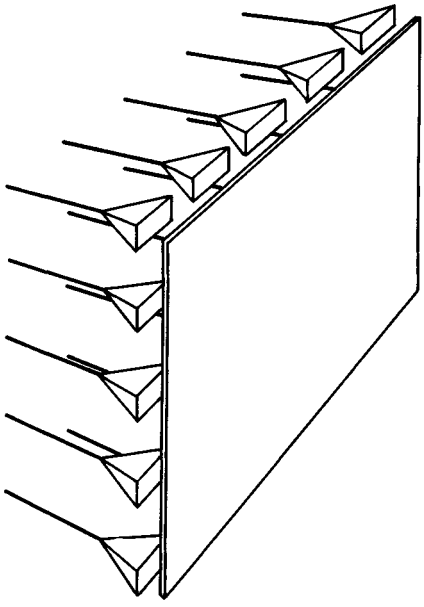

FIG. 7.21 Planar array with a thin dielectric sheet spaced a fraction of a wavelength from the radiators.

Small Arrays. The element pattern is the best single indicator of impedance matching in a scanning array. One way of determining the element pattern is to build a small array. A central element is excited, and all other elements are terminated. The pattern of this central element is the active element pattern.

Diamond[76] has examined the number of elements required in a small array to provide a reasonable approximation to an element in an infinite array. He concludes that 25 to 37 elements are required to provide a good indication. Figure 7.22 shows the change in the measured active element pattern as the number of elements is increased. For a 41-element array the null is very pronounced. Even for the 23-element array it is clear that the gain variation with scanning is dramatically greater than cos θ.

The small array can also be used to measure coupling coefficients as demonstrated by Fig. 7.12. These coupling coefficients can be used to calculate the impedance variation as the array is scanned. Grove, Martin, and Pepe[77] have noted that for the element to be matched in its operating environment the self-coupling C_{11} must exactly cancel the coupling from all other elements. They have used this technique to provide a good match on an ultralow-sidelobe, wideband phased array. After adjusting C_{11} to cancel the sum of the other mutuals, they further adjusted the amplitude of C_{11} to compensate for the variation in mismatch loss due to the resultant change in C_{11}. Results were obtained for an array of greater than two-octave bandwidth. In this design grating lobes were permitted to enter real space. At this point a high mismatch was observed. The mismatch improved as the grating lobe moved further into real space.

The combination of waveguide simulators and small arrays provides powerful empirical tools to supplement the analytical techniques. Experience has demonstrated that a large antenna should not be built until the element pattern has been verified with a small array.

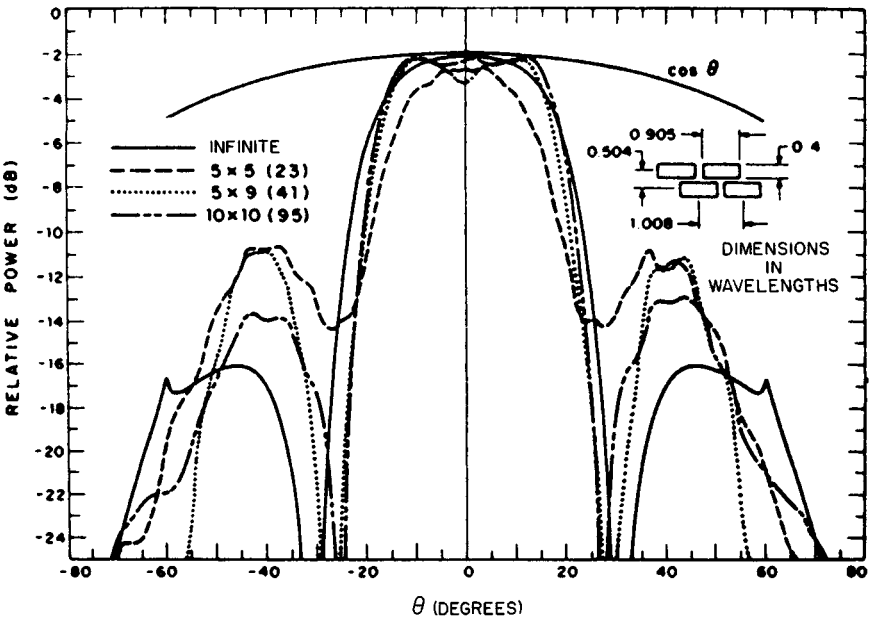

FIG. 7.22 Experimental *H*-plane patterns of the center elements of waveguide arrays. (*After Diamond.*[76])